

Supplementary Note A: Hamiltonian of the superconducting quantum simulator

In this section, we perform the circuit quantization of the superconducting architecture proposed in the main text. To do it more pedagogically, without loss of generality, we will focus in the description of the building block shown in Supplementary Fig. 1, whose Lagrangian reads

$$\mathcal{L} = \sum_{j=1}^2 \left[\frac{C_{g_j}}{2} (\dot{\Phi}_j - V_{g_j})^2 + \frac{C_{J_j}}{2} \dot{\Phi}_j^2 + E_{J_j} \cos(\varphi_j) \right] + E_{J_s}^{\text{eff}} \cos(\varphi_s) + \frac{C_s}{2} \dot{\Phi}_s^2 + \frac{C_c}{2} (\dot{\Phi}_1 - \dot{\Phi}_s)^2 + \frac{C_c}{2} (\dot{\Phi}_s - \dot{\Phi}_2)^2 \quad (\text{A1})$$

$$+ \frac{C}{2} \dot{\Phi}_R^2 + \frac{1}{2L} \Phi_R^2 + \frac{C_c}{2} (\dot{\Phi}_s - \dot{\Phi}_R)^2, \quad (\text{A2})$$

where $\varphi_j = 2\pi\Phi_j/\Phi_0$, with $\Phi_0 = h/2e$ is the superconducting flux quantum and $2e$ is the electrical charge of a Cooper pair, and $E_{J_s}^{\text{eff}} = 2E_{J_s} \cos(\varphi_{\text{ext}})$ is the effective Josephson energy of the SQUID. Now, we calculate the conjugate momenta (node charge) $Q_j = \partial L / \partial \dot{\Phi}_j$ obtaining

$$\begin{aligned} Q_{1(2)} &= C_{g_{1(2)}} (\dot{\Phi}_{1(2)} - V_{g_{1(2)}}) + C_{J_{1(2)}} \dot{\Phi}_{1(2)} + C_c (\dot{\Phi}_{1(2)} - \dot{\Phi}_s) \\ Q_s &= C_s \dot{\Phi}_s - C_c (\dot{\Phi}_1 - \dot{\Phi}_s) - C_c (\dot{\Phi}_2 - \dot{\Phi}_s) + C_c (\dot{\Phi}_s - \dot{\Phi}_R) \\ Q_R &= C \dot{\Phi}_R - C_c (\dot{\Phi}_s - \dot{\Phi}_R), \end{aligned} \quad (\text{A3})$$

The classical Hamiltonian is obtained by applying the Legendre transformation $\mathcal{H}(\Phi_k, Q_k) = \vec{Q}_k^\top \vec{\dot{\Phi}}_k - \mathcal{L}$, obtaining

$$\begin{aligned} \mathcal{H} &= \sum_{j=1}^2 \left[\frac{1}{2\tilde{C}_j} (Q_j + \tilde{Q}_j)^2 - E_{J_j} \cos(\varphi_j) \right] + \left[\frac{1}{2C_7} Q_s^2 - E_{J_s}^{\text{eff}} \cos(\varphi_s) + \frac{1}{2C_9} Q_R^2 + \frac{1}{2L} \Phi_R^2 \right] + \frac{1}{2} \left[\frac{2}{C_2} Q_1 Q_2 + \frac{2}{C_3} Q_1 Q_s + \frac{2}{C_5} Q_2 Q_s \right. \\ &\quad \left. + \frac{2}{C_4} Q_1 Q_R + \frac{2}{2C_6} Q_2 Q_R + \frac{2}{C_8} Q_R Q_s + \frac{2}{C_2} \tilde{Q}_1 Q_2 + \frac{2}{C_2} Q_1 \tilde{Q}_2 + \frac{2}{C_2} \tilde{Q}_1 \tilde{Q}_2 + \frac{2}{C_3} \tilde{Q}_1 Q_s + \frac{2}{C_4} \tilde{Q}_1 Q_R + \frac{2}{C_5} \tilde{Q}_2 Q_s + \frac{2}{C_6} \tilde{Q}_2 Q_R \right] \end{aligned} \quad (\text{A4})$$

where, $\tilde{C}_1 = \tilde{S}_c / [\tilde{C} (\tilde{C}_s C_{\Sigma 2} - C_c^2) - C_c^2 C_{\Sigma 2}]$, $\tilde{C}_2 = \tilde{S}_c / [\tilde{C} (\tilde{C}_s C_{\Sigma 1} - C_c^2) - C_c^2 C_{\Sigma 1}]$, $C_2 = \tilde{S}_c / C_c^2 \tilde{C}$, $C_3 = \tilde{S}_c / \tilde{C} C_c C_{\Sigma 2}$, $C_4 = \tilde{S}_c / C_c^2 C_{\Sigma 2}$, $C_5 = \tilde{S}_c / \tilde{C} C_c C_{\Sigma 1}$, $C_6 = \tilde{S}_c / C_c^2 C_{\Sigma 1}$, $C_7 = \tilde{S}_c / \tilde{C} C_{\Sigma 1} C_{\Sigma 2}$, $C_8 = \tilde{S}_c / C_c C_{\Sigma 1} C_{\Sigma 2}$, $C_9 = \tilde{S}_c / [C_{\Sigma 2} (\tilde{C}_s C_{\Sigma 1} - C_c^2) - C_c^2 C_{\Sigma 1}]$, $\tilde{Q}_1 = C_{g_1} V_{g_1}$ and $\tilde{Q}_2 = C_{g_2} V_{g_2}$, and C^{-1} is the inverse capacitance matrix. The offset terms have been neglected.

Using the approximations, $\dot{\Phi}_s \ll \dot{\Phi}_{1(2)}$ and $\Phi_s \ll \Phi_{1(2)}$, i.e. we consider the SQUID in the high plasma frequency regime, and low impedance. From the first approximation $\dot{\Phi}_s \ll \dot{\Phi}_{1(2)}$, we can approximate $\dot{\Phi}_{1(2)} - \dot{\Phi}_s \approx \dot{\Phi}_{1(2)}$ and since $C_s \sim C_{g_{1(2)}}$, we can approximate $C_c \dot{\Phi}_{1(2)} - C_s \dot{\Phi}_s \approx C_c \dot{\Phi}_{1(2)}$ in Eq. (A3), obtaining

$$Q_s = -C_c \left(\frac{Q_1 + \tilde{Q}_1}{C_{\Sigma 1}} + \frac{Q_2 + \tilde{Q}_2}{C_{\Sigma 2}} + \frac{Q_R}{C + C_c} \right) \quad (\text{A5})$$

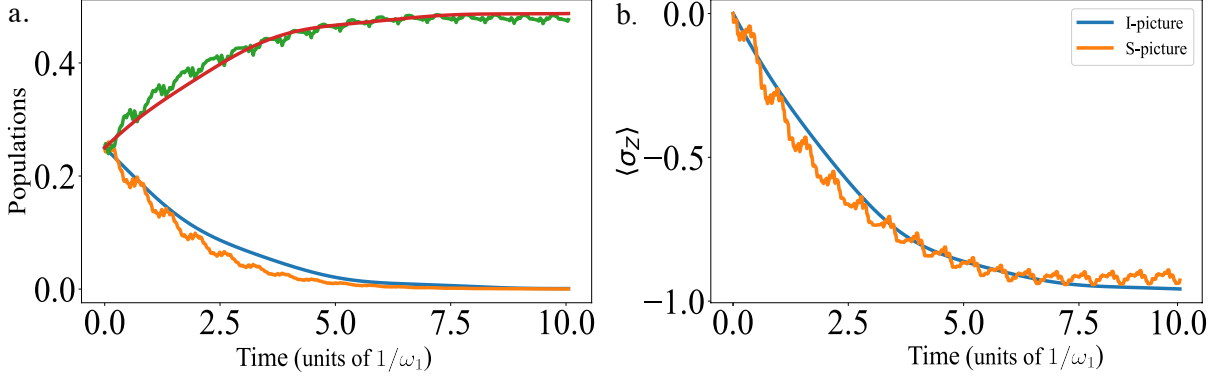
where, $\tilde{Q}_j = C_{g_j} V_{g_j}$. Using the Euler-Lagrange equation $\frac{d}{dt} \left(\frac{\partial \mathcal{L}}{\partial \dot{\Phi}} \right) - \frac{\partial \mathcal{L}}{\partial \Phi} = 0$, we obtain the relations

$$\begin{aligned} C_{g_{1(2)}} \ddot{\Phi}_{1(2)} + C_{J_{1(2)}} \ddot{\Phi}_{1(2)} + \frac{2\pi}{\Phi_0} E_{J_j} \sin(\varphi_j) + C_c (\ddot{\Phi}_{1(2)} - \ddot{\Phi}_s) &= 0 \\ C_s \ddot{\Phi}_s + C_c (-\ddot{\Phi}_1 - \ddot{\Phi}_2 - \ddot{\Phi}_R + 3\ddot{\Phi}_s) + \frac{2\pi}{\Phi_0} E_{J_s}^{\text{eff}} \sin \varphi_s &= 0 \\ C \ddot{\Phi}_R + C_c (\ddot{\Phi}_R - \ddot{\Phi}_s) - \frac{\Phi_R}{L} &= 0 \end{aligned} \quad (\text{A6})$$

where, we have used $\varphi_j = 2\pi\Phi_j/\Phi_0$. Considering the mentioned approximations, we obtain

$$\varphi_s = \frac{C_c}{E_{J_s}^{\text{eff}}} \left(-\frac{E_{J_1} \sin \varphi_1}{C_{g_1} + C_{j_1} + C_c} - \frac{E_{J_2} \sin \varphi_2}{C_{g_2} + C_{j_2} + C_c} + \frac{\Phi_0}{2\pi} \frac{\Phi_R}{L(C + C_c)} \right) \quad (\text{A7})$$

where, σ_j^y is the Pauli Y matrix. Since $\gamma_j^2(\varphi_{ext})(\sin \hat{\varphi}_j)^2$ is a constant term, we can ignore it as it only provides a shift to the



Supplementary Figure 2: We compare the curves corresponding to the effective dynamics given by Hamiltonian in Eq. (A17) and exact dynamics. a. Population of states $|000\rangle$ (orange) and $|001\rangle$ (green). b. Dynamics of $\langle \sigma_z \rangle$, initial state $|\psi\rangle = |\psi_1\rangle \otimes |\psi_r\rangle \otimes |\psi_2\rangle$, where $|\psi_i\rangle = \frac{1}{\sqrt{2}}(|0\rangle + |1\rangle)$ are the initial qubit states and $|\psi_r\rangle = |0\rangle$ is the initial state of the resonator. We use $k_0 = 0.08$, $l_0 = 0.02$ and $m_0 = 0.01$, $A_i/\varphi_{DC} = 0.1$, $\omega_1 = 1$, $\omega_2 = 0.9$ and $\omega_R = 0.6$ (frequencies are in units of $1/\omega_1$), and the phases are $\tilde{\varphi}_{QQ}^\pm = \pi$, $\tilde{\varphi}_{QR}^{\pm(j)} = 0$.

qubit frequency. Using these relations, the Hamiltonian is given by

$$\hat{\mathcal{H}} = \sum_{j=1}^2 \left[\frac{\omega_j}{2} \sigma_j^z - \frac{\omega'_j(\varphi_{ext})}{2} \sigma_j^y (\hat{a}^\dagger + \hat{a}) \right] + \left[\omega_R \left(a^\dagger a + \frac{1}{2} \right) + \frac{E_{Ls}(\varphi_{ext})}{2} \phi_R (\hat{a}^\dagger + \hat{a})^2 + \frac{E_{Js}^{\text{eff}} \gamma_1 \gamma_2 (\varphi_{ext})}{4} \sigma_1^y \sigma_2^y \right] \quad (\text{A13})$$

where, $\omega_j = \sqrt{8E_{Cj}E_{Jj}}$, $\omega'_j(\varphi_{ext}) = \frac{\Phi_0^2}{4\pi^2} \gamma_j(\varphi_{ext}) \frac{\phi_R}{L(\frac{C}{C_c} + 1)}$ and $\omega_R = \sqrt{8E_{LR}E_{CR}}$. We consider the external flux to be composed of a DC signal and a small AC signal, $\varphi_{ext} = \varphi_{DC} + \varphi_{AC}(t)$, where $\varphi_{AC}(t) = \varphi_R + \sum_\alpha \varphi_{QQ}^\alpha + \varphi_{QR}^{\alpha(1)} + \varphi_{QR}^{\alpha(2)}$, where $\alpha = \{+, -\}$ and $\varphi_{ab}^\alpha = A_{ab} \cos(\nu_{ab}^\alpha t + \tilde{\varphi}_{ab}^\alpha)$. Furthermore, for the case $|A_i| \ll 1$, we can approximate

$$\frac{1}{E_{Js}^{\text{eff}}} \approx \frac{1}{E_{Js}} \left[1 + \frac{\sin(\varphi_{DC})}{\cos \varphi_{DC}} \varphi_{AC}(t) \right] \quad (\text{A14})$$

where, $\bar{E}_{Js} = 2E_{Js} \cos \varphi_{DC}$. Using the Eq. (A14) in the Eq. (A13), we get

$$\hat{\mathcal{H}} = \left[\frac{\omega_1}{2} \sigma_1^z + \frac{\omega_2}{2} \sigma_2^z + \omega_R \left(a^\dagger a + \frac{1}{2} \right) \right] + \left[[k_0 + k_1 \varphi_{AC}(t)] (\hat{a}^\dagger + \hat{a})^2 + [m_0 + m_1 \varphi_{AC}(t)] \sigma_1^y \sigma_2^y - \sum_{j=1}^2 [l_0^j + l_1^j \varphi_{AC}(t)] \sigma_j^y (\hat{a}^\dagger + \hat{a}) \right] \quad (\text{A15})$$

where the coupling strengths are defined as

$$k_0 = \frac{\phi_R}{\bar{E}_{Js}} \left(\frac{\Phi_0^2}{4\pi^2 L(C/C_c + 1)} \right)^2, m_0 = \frac{1}{4\bar{E}_{Js}} \frac{E_{J1}E_{J2}}{\left(\frac{C_{g1}}{C_c} + \frac{C_{J1}}{C_c} + 1 \right)}, l_0^j = \frac{\Phi_0^2}{4\pi^2 \bar{E}_{Js}} \frac{\phi_R}{L \left(\frac{C}{C_c} + 1 \right)} \frac{E_{Jj}}{\left(\frac{C_{g1}}{C_c} + \frac{C_{J1}}{C_c} + 1 \right)},$$

$$k_1 = k_0 \tan(\varphi_{DC}), \quad m_1 = m_0 \tan(\varphi_{DC}), \quad l_1^j = l_0^j \tan(\varphi_{DC}) \quad (\text{A16})$$

With current state-of-the-art superconducting technologies [1] we can achieve the range $0 \leq l_1^j/g_0 \leq 6.8$. The parameter ranges for various components correspond to $C \approx 15 - 40 fF$, $C_c = C_g = 0.1C$ for the capacitors and coupling (or gate) capacitors, $L \approx nH$, for the inductors, $E_J = E_{Js} \approx 10E_c - 50E_c$ for the qubit and SQUID Josephson energies. To get the effective interactions, we can write the Hamiltonian in the interaction picture, considering as free Hamiltonian $\mathcal{H}_0 = \left[\frac{\omega_1}{2} \sigma_1^z + \frac{\omega_2}{2} \sigma_2^z + \omega_R \left(a^\dagger a + \frac{1}{2} \right) \right]$ and the interaction as $V = \left[[k_0 + k_1 \varphi_{AC}(t)] (\hat{a}^\dagger + \hat{a})^2 + [m_0 + m_1 \varphi_{AC}(t)] \sigma_1^y \sigma_2^y - \frac{1}{4} \sum_{j=1}^2 [l_0^j + l_1^j \varphi_{AC}(t)] \sigma_j^y (\hat{a}_j^\dagger + \hat{a}_j) \right]$. Finally we choose $\nu_{QQ}^\pm = \omega_1 \pm \omega_2$, $\nu_{QR}^{\pm(1)} = \omega_1 \pm \omega_R$, $\nu_{QR}^{\pm(2)} = \omega_2 \pm \omega_R$, and after a

Operator	$\tilde{\varphi}_{QQ}^+$	$\tilde{\varphi}_{QQ}^-$	$\tilde{\varphi}_{QR}^{+(L)}$	$\tilde{\varphi}_{QR}^{-(L)}$	$\tilde{\varphi}_{QR}^{+(R)}$	$\tilde{\varphi}_{QR}^{-(R)}$
$\sigma_{L,j}^x \sigma_{R,j}^x$	0	0	—	—	—	—
$\sigma_{L,j}^y \sigma_{R,j}^y$	0	π	—	—	—	—
$\sigma_{L,j}^x \sigma_{R,j}^y$	$\pi/2$	$-\pi/2$	—	—	—	—
$\sigma_{L,j}^y \sigma_{R,j}^x$	$\pi/2$	$\pi/2$	—	—	—	—
$\sigma_{L,j}^x (a + a^\dagger)$	—	—	$\pi/2$	$\pi/2$	—	—
$\sigma_{R,j}^x (a + a^\dagger)$	—	—	—	—	$\pi/2$	$\pi/2$
$\sigma_{L,j}^y (a + a^\dagger)$	—	—	$-\pi/2$	$\pi/2$	—	—
$\sigma_{R,j}^y (a + a^\dagger)$	—	—	—	—	$-\pi/2$	$\pi/2$
$\sigma_{L,j}^x (a - a^\dagger)$	—	—	0	0	—	—
$\sigma_{R,j}^x (a - a^\dagger)$	—	—	—	—	0	0
$\sigma_{L,j}^y (a - a^\dagger)$	—	—	π	0	—	—
$\sigma_{R,j}^y (a - a^\dagger)$	—	—	—	—	π	0

Supplementary Table I: Phase selection to mimic different interactions.

rotating wave approximation, neglecting the fast oscillation terms, we obtain the final effective Hamiltonian for each building block (site)

$$\begin{aligned}
H_s = & \frac{m_1 A_{QQ}}{4} \left[C_{QQ}^+ \sigma_{L,j}^x \sigma_{R,j}^x - S_{QQ}^+ \sigma_{L,j}^x \sigma_{R,j}^y + S_{QQ}^- \sigma_{L,j}^y \sigma_{R,j}^x + C_{QQ}^- \sigma_{L,j}^y \sigma_{R,j}^y \right] \\
& + \frac{1}{4} \sum_{\alpha=\{L,R\}} A_{QR} l_1^\alpha \left[C_{QR}^+ \sigma_{\alpha,j}^x (a_j^\dagger - a_j) - C_{QR}^- \sigma_{\alpha,j}^y (a_j^\dagger + a_j) + S_{QR}^+ \sigma_{\alpha,j}^x (a_j^\dagger + a_j) - S_{QR}^- \sigma_{\alpha,j}^y (a_j^\dagger - a_j) \right],
\end{aligned} \tag{A17}$$

we have replaced the index $1(2) \rightarrow L(R)$ to refer to the qubit left and right of each building block. Also we have defined $C_{ab}^\pm = \cos \tilde{\varphi}_{ab}^+ \pm \cos \tilde{\varphi}_{ab}^-$, and a similar definitions for S_{ab}^\pm by replacing sin by cos. We compare the dynamics of the Schrödinger and Interaction picture Hamiltonians in the plots shown in Supplementary Fig. 2. The results of the population of states and the dynamics of the Pauli σ_z operator of both pictures coincide well.

Following the same procedure we can derive the Hamiltonian to couple adjacent building blocks which reads

$$H_{s-s}^{(j)} = \frac{m_1 \bar{A}_{QQ}}{4} \left[C_{\phi QQ}^+ \sigma_{R,j}^x \sigma_{L,j+1}^x - S_{\phi QQ}^+ \sigma_{R,j}^x \sigma_{L,j+1}^y + S_{\phi QQ}^- \sigma_{R,j}^y \sigma_{L,j+1}^x + C_{\phi QQ}^- \sigma_{R,j}^y \sigma_{L,j+1}^y \right] \tag{A18}$$

where $\tilde{C}_{ab}^\pm = \cos \tilde{\varphi}_{ab}^+ \pm \cos \tilde{\varphi}_{ab}^-$, and S_{ab}^\pm is obtained by replacing sin by cos.

[1] G. Wendin, *Quantum information processing with superconducting circuits: a review*, *Rep. Prog. Phys.* **80** (2017).